

Sonoluminescence optical confocal tomography of tissue

Yonghong He¹, Da Xing¹, Yong Yao¹, Ken-ichi Ueda²

¹ Institute of Laser Life Science, South China Normal University, Guangzhou 510631, P. R. China

² Institute of Laser Science, University of Electro-Communications, 1-5-1 Chofugaoka, Chofu, Tokyo 182-8585, Japan

Abstract: In this paper, we report experiments on optical confocal tomography by use of sonoluminescence signal in both biological tissue and tissue-simulating media. A high-sensitive confocal scanning setup based on photon counting technique was developed. With the system, we obtained images of the objects embedded in tissue-simulating turbid media. The images showed a high contrast and a lateral resolution of about 100 μm . We finally imaged a carbon stick buried in muscle tissue with the sonoluminescence confocal scanning tomography. This technique has potential applications in clinical diagnosis.

Key words: Sonoluminescence – tissue – confocal tomography

1. Introduction

Sonoluminescence (SL) has attracted more and more attention in this decade [1–6]. SL arises from the cavitation process, in which bubbles filled with gas and vapor are generated within the liquid under ultrasonic action. Hilgenfeldt et al. [1] considered that SL was generated by thermal bremsstrahlung and recombination radiation when bubbles collapsed. Recently Wang and Shen [4] reported a technology of sonoluminescent tomography in strongly scattering media, and predicted its potential applications in medical diagnosis. Advantages of SL tomography are high signal-to-noise ratio owing to the internally generated signal, high imaging contrast owing to multiple contrast sources and low cost of equipment for application.

The present SL imaging technique includes high-sensitive CCD surface imaging [5] and focal ultrasonic scanning tomography [6]. With the former technique, one can not get a tomographic image. In the later technique, the spatial resolution is limited by the ultrasonic focal size of about several millimeters, especially the ultrasonic axis direction of about 6 millimeters or more at 1 MHz frequency [7]. The ultrasonic power intensity at the focal site is often larger than the damage threshold of tissue.

In this paper, we propose an optical confocal tomography by use of SL. We first report experiments on SL confocal scanning tomography of objects buried in both biological tissue and tissue-simulating media. With this technique, the imaging spatial resolution was largely improved to about 100 micrometer with the ultrasonic intensity far less than the safety limit of 23-bar set by US FDA.

2. Materials and methods

The experimental apparatus is shown in fig. 1. A function generator (Tektronics, AFG320) produces a 1 MHz sinusoidal signal, and then a power amplifier (ENI Co. Ltd, 2100L) amplified the signal to drive the ultrasonic transducer (3 cm in diameter, Meza Guangzhou, China). The measurements with a PVDF hydrophone (HPM1/1, Precision Acoustics) showed that the ultrasound field is column-shape and the peak-peak pressure at the location of the sample is 2.0 bars. An objective lens with a working distance of 1.5 cm (BioRad, NA 0.4) is used to collect SL from the sample. A pinhole with 200 μm in diameter is put on the plane 15 cm from the lens to select the light from a confocal point of the sample. The light through the pinhole is detected by a photomultiplier tube (CR-129, Hamamatsu, Beijing), which is biased at -1200 V and cooled to -20° to reduce the thermal noise. The signal from the PMT is amplified by a preamplifier ($\times 5$) and a main amplifier ($\times 100$, Beijing Nuclear Industrial Co. Ltd., China). Then a discriminator thresholded at 1 V convert the signal to TTL pulses. The pulses are counted by a multi-function I/O card (PCL-818LS, Advantech Co. Ltd.), which is directly plugged in the ISA bus of the personal computer. The counter reading and data processing was performed by the LabVIEW software (National Instrument, Version 5.1). The computer also controls the scanning of the two-dimensional translation stage through the I/O card. During raster scanning of the stage, which was fixed with the pool and the ultrasonic transducer, in the $x - y$ plane with a step size of 0.1 mm, the personal computer counted the signal pulses of SL versus the values of x , y . Two-dimensional images of the objects buried in the scatter-

Received 3 January 2002; accepted 8 May 2002.

Correspondence to: D. Xing
Fax: ++86-20-85216052
E-mail: heyh@sncu.edu.cn

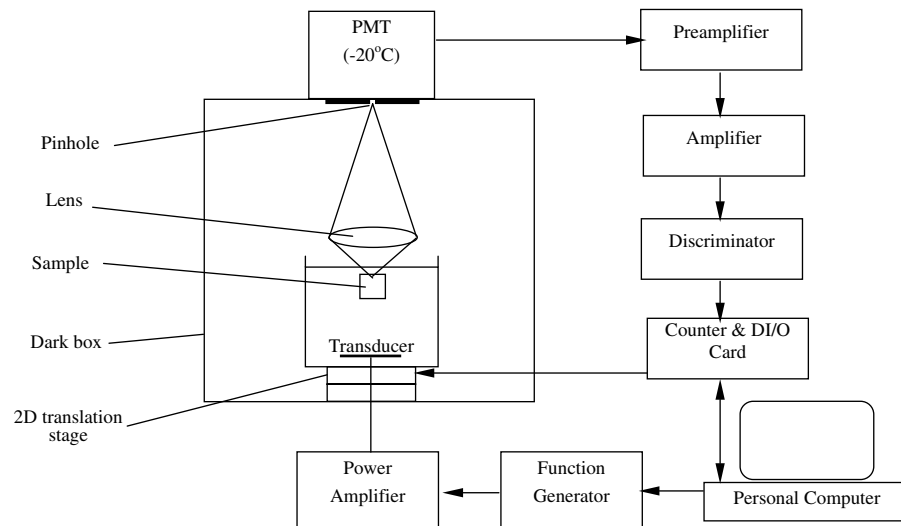


Fig. 1. A schematic diagram of experimental setup.

ing media were plotted with the counts data. The value of counts represents an integrated SL intensity from the confocal point of the pinhole with a time constant of 5 s. In the integrated SL measurement experiments, the PMT worked in direct current (DC) way because the signal is relatively strong. The DC signal from the PMT is directly acquired by the multi-function card (12 bit A/D resolution). The value of DC voltage represents a time-averaged biological SL intensity with a time constant of 1 s.

We prepared the tissue simulation phantom by mixing 8 ml dominantly scattering Intralipid (Pharmacia) and 3.25×10^{-8} mol Trypan Blue (Sigma) in 360 ml distilled water. At the wavelength of 584 nm, which is the absorption peak of Trypan Blue dye, the reduced scattering coefficient μ'_s and the absorption coefficient μ_a of the phantom were 6.15 cm^{-1} and 0.014 cm^{-1} , respectively. The optical property of the phantom is comparable with that of biological tissue [8–9]. A carbon object with a side length of 1.0 mm was buried in the phantom. The height between the upper plane of the objects and the surface of the phantom was 3 mm. Fresh porcine muscle tissues were cut into slices of $20 \times 20 \times 10 \text{ mm}$. A carbon stick ($0.5 \text{ mm} \times 5 \text{ mm}$) was buried in the tissue 3 mm under the surface for imaging. In some experiments, FCLA (Tokyo Kasai Co. Ltd.), which is a chemiluminescence reagent and can work in vivo [10, 5], was dissolved in saline ($5 \mu\text{mol/L}$) and injected into the phantom 1 min before measurement.

3. Results and discussions

We measured the relation between the SL intensity and the peak-peak voltage applied to the ultrasonic transducer in the tissue-simulating media and the porcine muscle, liver and fat tissues (fig. 2). The ultrasonic pressure was proportional to the peak-peak voltage ap-

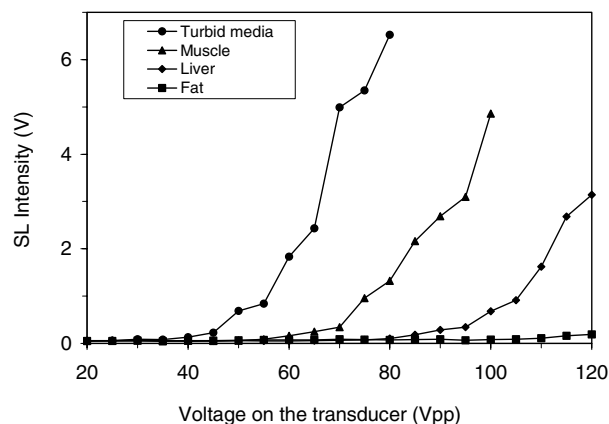


Fig. 2. Effect of the driving voltage on the ultrasonic transducer on the SL intensity from the tissue-simulating media and porcine muscle, liver and fat tissues.

plied to the transducer. Because of the limitation of power on the ultrasonic transducer, we could not measure the SL in fat tissue with the present acoustic pressure. The result showed clearly that there were thresholds of ultrasonic pressure to generate SL in the muscle, liver tissues and the media. The thresholds are in the order: liver > muscle > scattering media. It is difficult to generate SL in SL from tissue than from the media because of the different environment and the water status. Because of the limitation of power on the ultrasonic transducer, we could not measure the upper ultrasonic thresholds, although there must have been some. When the ultrasonic pressure increased above the threshold, the SL intensity increased rapidly with the pressure. The SL intensity of tissue is lower than that of the media when the same pressure is applied. The rapid increase of the SL intensity with the acoustic pressure above the thresholds indicated that the SL signal would be a sensitive measure of tissue imaging.

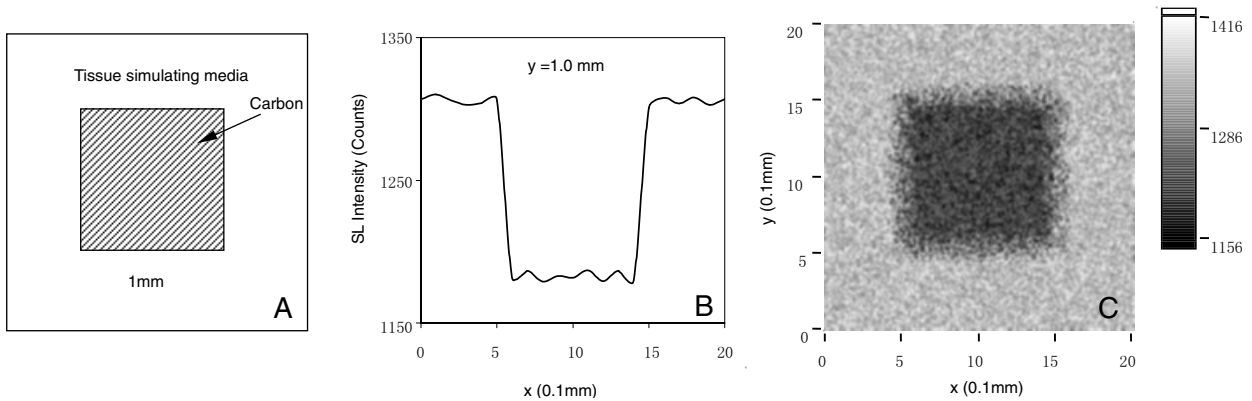


Fig. 3. a) Schematic diagram of a cubic object (1 mm side length) buried in the Intralipid phantom. b) One dimensional SL intensity graph horizontally across the center of the object (parallel with the x axis at $y = 1.0$ mm). c) $x - y$ plane two dimensional SL image of the object in the Intralipid phantom.

The 100V peak-peak voltage, corresponding to ultrasonic pressure of 2.0 bars, was applied in the following imaging experiments. A carbon cube embedded in the Intralipid phantom was imaged with SLT (fig. 3). The schematic of the object buried in the Intralipid phantom is shown in fig. 3a. Firstly, we scan the simulating medium with the object along x -axis direction, the horizontal line in tomographic plane, one-dimensional distribution of SL intensity signal can be plotted as fig. 3b. Then, scanning along both x -axis and y -axis, we can obtain two-dimensional distribution of this signal intensity and reconstruct a tomographic image (fig. 3c) of buried cube in dense turbid medium. fig. 3c shows that the contrast of the image is excellent and the boundary of the object is clear. The average counts of the tissue-simulating phantom is 1380 counts, while that of carbon region is 1120 counts. The contrast of the SL images was based on the difference between the optical and the ultrasonic properties of the objects and those of the surrounding medium. The object was optically opaque,

ultrasonically absorbing and yielded no SL signal, while the simulating medium was optically scattering, ultrasonically transparent and produce SL. So when the pin-hole confocal point falls on the object, the SL intensity dropped quickly.

To observe the spatial resolution of the system, we buried a “□” quadrate shape objects in the Intralipid phantom with FCLA solution, the length of internal side is 0.2 mm and external side 1.2 mm. Two-dimensional sectional image was obtained as fig. 4b. fig. 4a is schematic diagram of the object buried in the phantom. The internal and external quadrate of the “□” shape object could be distinguished clearly with the correct shape and size. In the SL confocal tomography, the spatial resolution of the image is limited by the intensity of the SL. It is determined by the size of the pinhole and the imaging magnification. Because SL intensity is not much strong, the 200 μm pinhole size was selected to measure the SL signal in present experiment. The spatial resolution of the present system is estimated to 100 μm .

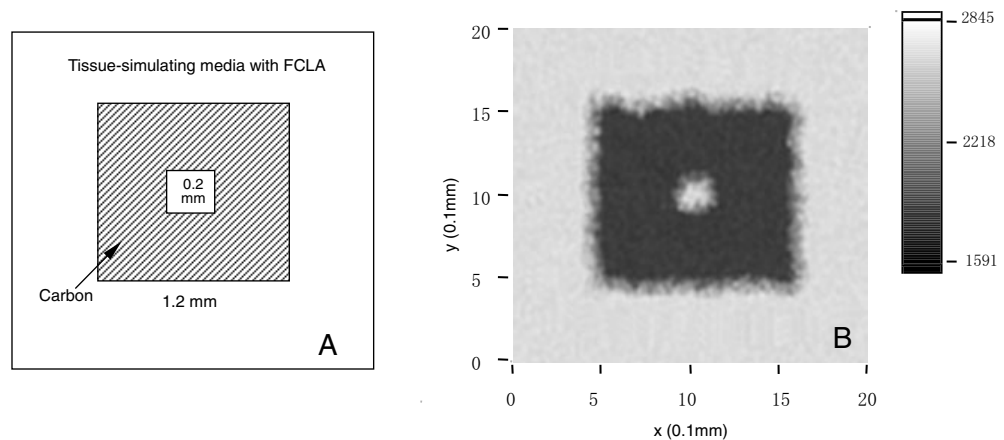


Fig. 4. a) Schematic diagram of “□” quadrate shape objects buried in the Intralipid phantom with FCLA solution; b) $x - y$ plane two dimensional SL image of the object in the Intralipid phantom with FCLA solution.

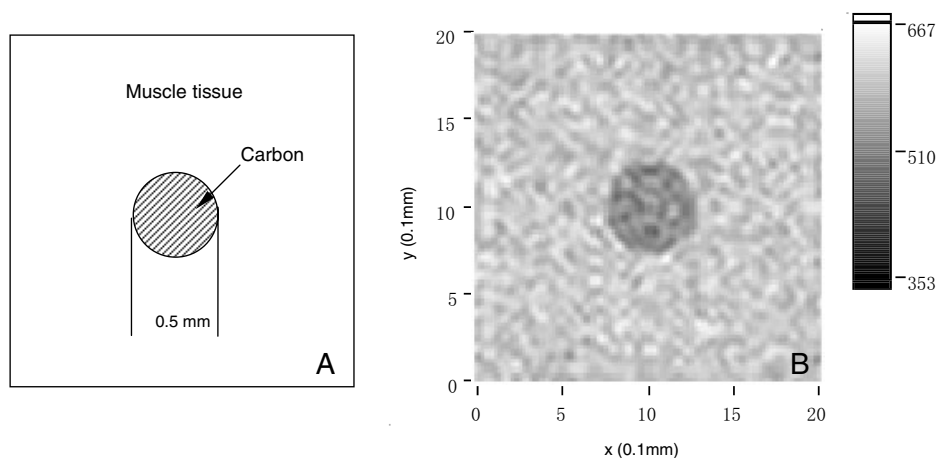


Fig. 5. a) Schematic diagram of a carbon stick (0.5 mm in diameter) buried in the muscle tissue; b) $x - y$ plane two dimensional SL image of the stick in the muscle tissue.

We choose the porcine muscle to do tissue SL confocal tomography. The schematic diagram of a carbon stick buried in the tissue is shown in fig. 5a. A two-dimensional SL confocal scanning image of the carbon stick is shown in fig. 5b. Although the SL intensity in tissue is relatively low (average 560 counts), fig. 5b shows the correct shape and size of the carbon stick. A good imaging contrast could be observed from the image.

The ultrasonic power density in the experiment is about 1.3 W/cm^2 , which is higher than the cavitation threshold but much lower than the damage threshold of the tissue lesion [11]. The present ultrasonic peak pressure was measured to be about 2 bars which is far less than the safety limit of 23 bars set by US FDA. The pressure could be in the safety window within which SL tomography can be achieved without cause of tissue damage [6].

4. Conclusions

SL optical confocal scanning tomography was used to image objects buried in both biological tissue and dense tissue-simulating turbid media. Both the spatial resolution and the contrast of the images were quite good. The spatial resolution of the image was largely improved to about 100 micrometer. The SL optical tomography has potential applications in clinical diagnosis.

Acknowledgements. This research is supported by the National Science Fund for Distinguished Young Scholars of China (No. 69725009), and the Team Project of Natural Science Foundation of Guangdong Province (No.015012).

References

- [1] Hilgenfeldt S, Grossmann S, Lohse D: A simple explanation of light emission in sonoluminescence. *Nature* **398** (1999) 402–405
- [2] Moss WC, Clarke DB, Young DA: Calculated pulse widths and spectra of a single sonoluminescing bubble. *Science*. **276** (1997), 1398–1401
- [3] Crum LA: Sonoluminescence. *Physics Today* **47** (1994) 22–29
- [4] Wang LV, Shen Q: Sonoluminescent tomography of strong scattering media. *Opt. Lett.* **23** (1998) 561–563
- [5] He Y, Xing D, Tang Y, Tan, S: Study on sonoluminescence imaging of living body. *ACTA OPTICA SINICA*, **21** (2001) 509–512
- [6] Shen Q, Wang LV: Two-dimensional imaging of dense tissue-simulating turbid media by use of sonoluminescence. *Appl. Opt.* **38** (1999) 246–252
- [7] Ying CF: *Ultrasonics*. Chinese Scientific Publishing House, Beijing 1990
- [8] Cheong WF, Prahl SA, Welch AJ: A review of the optical properties of biological tissues. *IEEE J. Quantum Electron.* **26** (1990) 2166–2185
- [9] van Staveren HJ, Moes CJM, van Marie J, Prahl SA, van Gemert MJC: Light scattering in Intralipid-10% in the wavelength range of 400–1100 nm. *Appl. Opt.* **30** (1991) 4507–4514
- [10] Nakano M: Detection of active oxygen species in biological systems. *Cellular and Molecular Neurobiology* **18** (1998) 565–579
- [11] Fry FJ, Sanghvi NT, Foster RS, Bihrl R, Hennige C: Ultrasound and microbubbles: their generation, detection and potential utilization in tissue and organ therapy – experimental. *Ultrasound Med. Biol.* **21** (1995) 1227–1237